

Large-Scale, Low-Amplitude Bedforms (Chevrons) in the Selima Sand Sheet, Egypt

TED A. MAXWELL AND C. VANCE HAYNES, JR.

Landsat images of the Selima sand sheet in southwestern Egypt display alternating light and dark chevron-shaped patterns that occur downwind from low scarps and major dune fields. Images acquired between 1972 and 1988 indicate that these features move as discrete bedforms at a rate of up to 500 meters per year. Extremely long-wavelength (130 to 1200 meters), low-amplitude (10 to 30 centimeters) bedforms were measured in the field; the light chevrons seen in the orbital data may be thin accumulations of active sand sheet deposits in the lee of these bedforms. Dark chevrons contain an admixture of coarse-granule lag deposits that are continually winnowed by aeolian erosion on the windward sides of the large bedforms. Sediment transport budgets derived from orbital and field analyses suggest net movement of up to 83,000 cubic meters per year for a single light chevron; such measurements can be used as a check on similar calculations from dunes and other smaller scale features to determine sand transport budgets for large areas of the eastern Sahara.

THE SELIMA SAND SHEET COVERS 100,000 km² of southwestern Egypt and northern Sudan (Fig. 1) (1) and consists of a barren, featureless plain of bimodal sand and coarse granules overlying alluvium with paleosols of varying stages of development (2). During our study of the Selima sand sheet, we observed chevron-shaped light- and dark-toned streaks in Landsat images, but we were unable to identify any features on the ground that could be responsible for the albedo contrast (3). In 1985, using a 1972 Landsat image for navigation, we made a detailed longitudinal traverse to sample the light and dark areas of these "chevrons." Variations in grain size and lithology were not apparent in the field, even after repeated traverses. Consequently, we acquired new image data to determine whether the patterns were still there. Visual comparisons of 1972 and 1986 Landsat Multispectral Scanner (MSS) scenes indicated that not only had some of the chevrons moved, but others had simply disappeared. On the basis of further field studies in an area of discrete chevron patterns and new orbital data acquired in 1988, we now suggest that these features are thin bedforms created by migration of active sand and remobilization of the upper surface of large-scale, low-amplitude bedforms in the sand sheet.

As depicted in Landsat MSS images (at 80-m spatial resolution), chevron patterns consist of irregularly spaced, light-toned, 0.5- to 2.0-km wide streaks oriented generally transverse to the dominant northerly wind direction, but with acute angles that

create an en-echelon, or chevron pattern (Fig. 2). Spacing between individual chevrons varies from 0.5 to 6 km, with a mean of 3.0 km, and although the features become more distinct in a downwind direction, there is no consistent variation of spacing downwind. The region of chevrons in the western part of the Selima sand sheet is bordered on the west by a dark, manganiferous, iron-rich sandstone surface and on the east by giant ripples with amplitudes of up to 10 m and wavelengths of about 500 m (4). Because of the distinct appearance of the chevrons at the western edge of the Selima sand sheet, we chose this area for detailed field and remote sensing investigations.

To determine changes between 1972 and 1988, we geometrically corrected and registered the 1972, 1986, and 1988 scenes by using default corner coordinates for the 1986 scene to map 10,000-km² subsets of the data into the UTM (Universal Transverse Mercator) ground coordinate system at a resampled pixel size of 50 m (5). Because of the lack of absolute ground control points, especially in the sand sheet where changes in albedo were observed, we used prominences on low bedrock ridges and barchan dunes as tie points.

We referenced field survey lines and sampling locations determined by multiple satellite fixes to the registered images by determining the offset between stable ground positions that could be seen in the images and recalculating the coordinates of the image data. We estimate that the cumulative error in these procedures is less than 200 m, which, in this area of extensive, homogeneous sand sheet cover, suggests that surface sampling is representative of the orbital depiction of reflectance variation.

We performed a radiometric calibration of the 1972, 1986, and 1988 images by

considering the differences in gains and offsets between the Landsat 1, 4, and 5 MSS sensors and calculating the radiance for each band (6). We normalized for solar irradiance by taking into account differences in sun angle and in sun-Earth distance between the acquisition times of each scene in order to compare absolute reflectance between the images (7). All images are cloud free, and we assume that atmospheric conditions were similar during the times each image was acquired. Several seasons of fieldwork during the fall and winter indicate that near-ground haze rarely occurs during the winter.

The location and appearance of chevrons changed during both a short-term (2.7-year) and long-term (16-year) period for which orbital remote-sensing data are available. Such changes consisted of (i) migration of discrete chevrons in a downwind (southerly) direction and (ii) appearance of new, light-toned chevrons and disappearance of some which had been present in 1972. Using images obtained in January 1986 and October 1988, we measured movement of 1400 m for individual light chevrons that retained their shape (Fig. 3), suggesting an annual rate of movement of 500 m per year. Using analog images at 1:1,000,000 scale, we had previously measured an annual rate of 100 m per year on the basis of a comparison of images acquired between 1984 and 1986 (8), although these earlier estimates are subject to greater error because of the scale of the images. The true migration rate most likely is somewhere between the two values. Digital comparisons of the 1972 and 1986 data indicate that some light-toned chevron patterns in the 1972 images did not com-

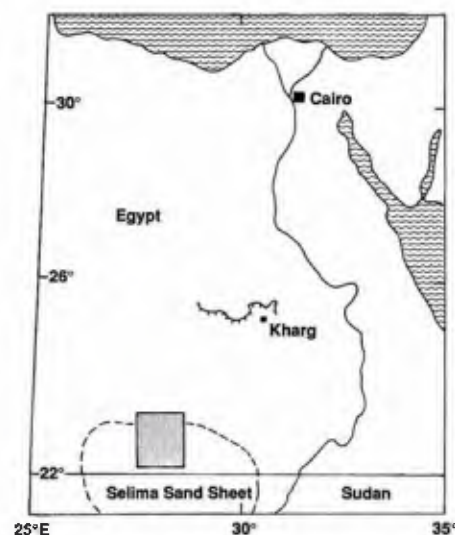


Fig. 1. Location of Selima sand sheet, southern Egypt and northern Sudan. Box outlines detailed area of remote sensing and field studies of large-scale bedforms and reflectance changes shown in Fig. 2.

T. A. Maxwell, Center for Earth and Planetary Studies, National Air and Space Museum, Smithsonian Institution, Washington, DC 20560.

C. V. Haynes, Jr., Departments of Anthropology and Geosciences, University of Arizona, Tucson, AZ 85721.

pletely disappear by 1986, but remained as a faint outline barely visible above the noise level of the image data (Fig. 4).

Differences in reflectance values between light and dark chevrons are extremely small (1 to 3%); if the patterns were not spatially coherent, such minor variations would be indistinguishable from normal brightness variations in the surrounding sand sheet. Comparison of the reflectance of light and dark chevrons in three bands (MSS 1, 3, and 4) of the 1972 and 1986 Landsat images indicates that dark chevrons became brighter and some light chevrons showed little apparent change (Fig. 5). Overall reflectance was extremely high for the sand sheet, approaching 0.50 in the near infrared.

During the 1985 through 1988 field seasons, we sampled and systematically photographed surfaces representative of broad (several hundred square meters) areas of the sand sheet. The difference between light and dark chevrons in the topmost layer of sand sheet deposits (the uppermost 0.5 cm) is that areas of dark chevrons contained a few percent of subrounded to rounded, 3.5- to 4.5-mm granules, equal to about 10 weight percent of the bulk sample. These dark, iron-stained granules were in a matrix of coarse sand-size particles that were compositionally indistinguishable from the grains in areas of light chevrons (9), and the grain size distribution of sands from areas of both light and dark chevrons showed the bimodality that is

typical of sand sheet deposits (10).

Although the coarser grain size of the dark granules may contribute to the lower reflectance of the dark chevrons, we believe that their different composition is more important. Shadows cast by the larger grains could contribute because a spherical grain 0.4 mm in diameter would cast only a 0.4-mm shadow on a planar surface under the nominal 45° sun elevation at the time of the Landsat passes during late fall and winter. However, both the glancing sun angle on the top surface of the grains and the surrounding matrix of 0.1- to 0.2-mm grains suggest that little true shadowing is present. In addition, a compositional difference between the light and dark chevrons is suggested in that the reflectance changes are nonlinear with wavelength (Fig. 5).

Our field surveys of the sand sheet indicate that this area is characterized by extremely long wavelength, low amplitude bedforms that are generally detected only with a laser theodolite with an accuracy of 5

Fig. 2. Landsat multi-spectral scanner (MSS) scene (band 4) of areas of large-scale bedforms and chevron patterns detected from orbit. Dune-fields to the west of the chevrons and low bed-rock outcrops north of this area provided control for geometric registration of 1972, 1986, and 1988 scenes.

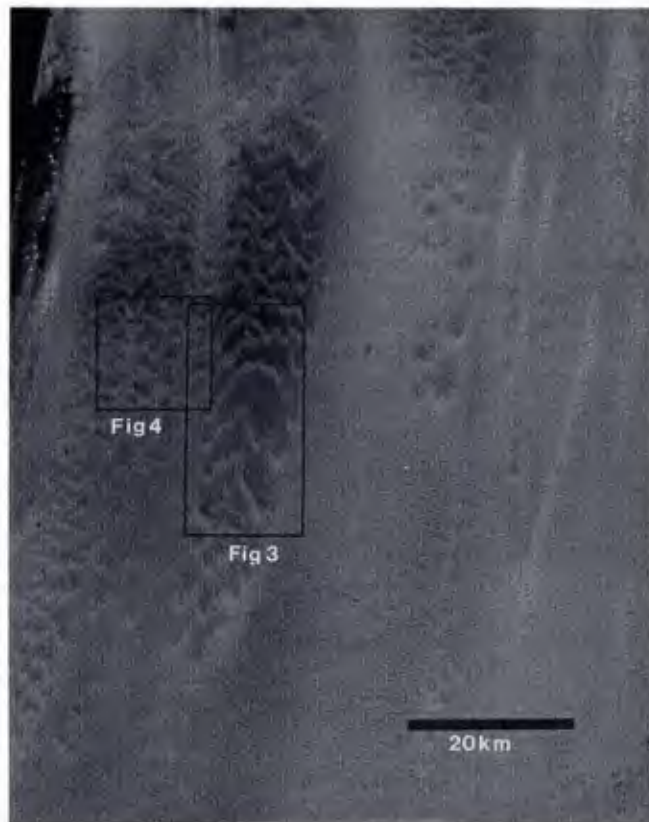


Fig. 3. Composite of band 4 MSS images taken in 1986 (Left) and 1988 (Right) showing movement of light chevrons over a 2.7-year period. The light patterns have retained their shapes, and have migrated 1.4 km southward during this time period.

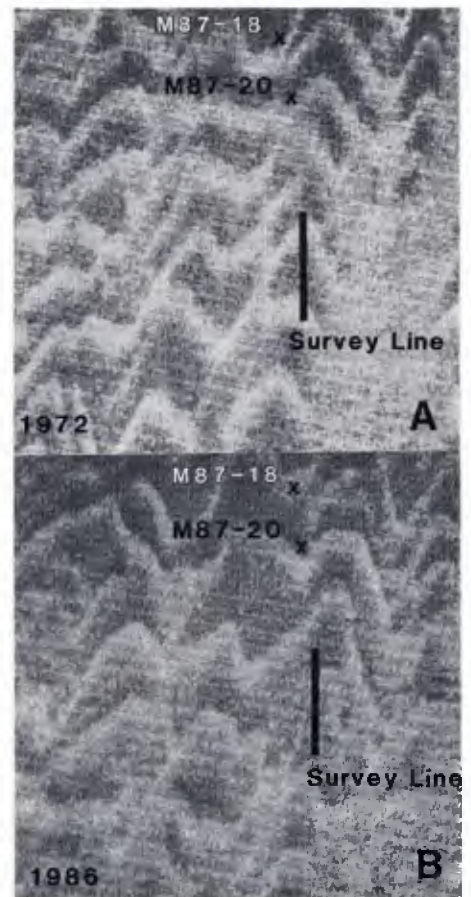
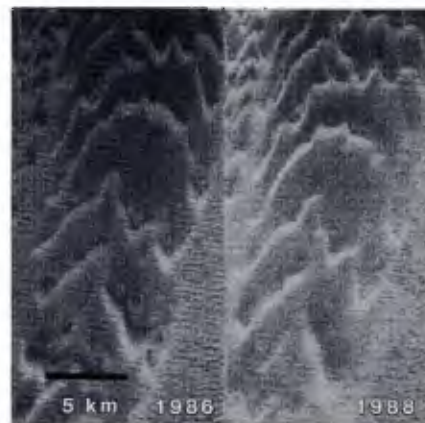


Fig. 4. (A) 1972 Landsat MSS 4 image showing two of the sample sites used for comparison with orbital data, and the location of the 2.7-km survey line across the light chevrons. (B) Same area as seen in 1986; chevrons have migrated from their prior position, and only a faint light trace of the 1972 bright streak remains at the northern end of the survey line.

mm. Two survey lines were made during 1987 and 1988, a 130-m line transecting a low bedform visible in the field (Fig. 6), and a 2.7-km line transecting one of the chevrons visible in the 1972 image, but greatly subdued in the 1986 data (Fig. 4). We measured elevations at 10- to 20-m intervals, and at each station, dug a 20- to 40-cm test pit to determine the subsurface stratigraphy.

The overall shape of the bedform surveyed in the 130-m line was asymmetric, in contrast to that of most small-scale ripples (11). Although a 100-m long form could be considered as a transverse dune, the steeper slope is on the stoss side (opposite the case of transverse dunes where the lee slope is steep), and the amplitude of 10 to 30 cm is

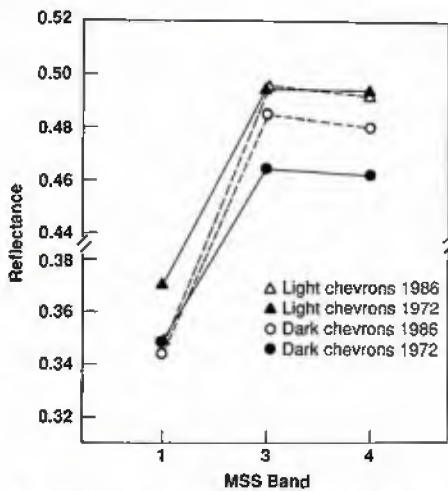


Fig. 5. Three-point spectral curves for areas of light and dark chevrons. Brightening of dark chevron areas occurred, but is not linear with spectral band, suggesting that compositional variations are the cause of reflectance differences.

an order of magnitude less than that of normal transverse dunes. The low relief bedform shown in Fig. 6 had a 10- to 15-cm thick layer of active sand sheet on its lee side, and in contrast to foreset beds of typical dunes, the primary stratification was planar, with alternating fine sand and granule layers typical of sand sheet deposits. Similar bedforms with amplitudes of 4 to 8 cm and wavelengths of 130 to 180 m were apparent in the longer survey line, where they were recognized from the thickening of active layers of sand sheet associated with minor topographic variations.

In addition to the 130- to 180-m bedforms, we identified even wider-spaced bedforms with wavelengths of 800 to 1200 m, within the range of the chevron patterns detected in the orbital data. Amplitudes varied from 15 to 30 cm, and two shorter wavelength forms were superposed on the northernmost crest of the larger bedform (Fig. 6). The crests of the long wavelength bedforms had 3 to 5 cm of active sand sheet deposits that thickened to 5 to 15 cm on the lee side. Beneath these deposits were older, pedogenesized sand sheet deposits that lacked primary planar stratification but had a bimodal sediment size distribution (2). The cores of the bedforms on the 1987-1988 transect consisted of calcified, fine pebble-gravel alluvium (cpg) set in a matrix of coarse silt- to sand-size grains. The topography of the upper contact of the cpg mimics the surface variations, with amplitudes of 10 to 15 cm, and between the bedforms, cpg was found in some areas at depths of 30 to 40 cm.

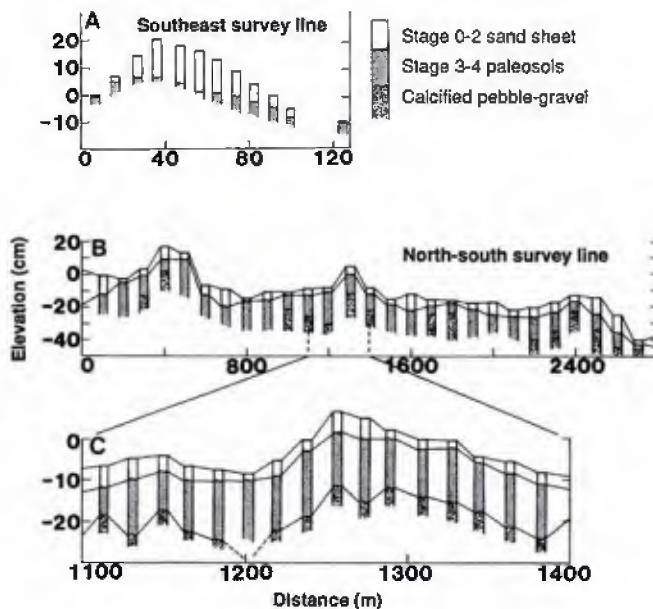
On the basis of our field surveys and remote sensing data, we interpret the light chevrons seen at orbital heights to be areas

of active sand sheet deposits that cover the coarse, ferruginous granule component prevalent in the areas of the dark chevrons. Because of the difficulty of identifying any topographic variations associated with light chevrons in the field, we are not certain that the large scale of these features is the result of single bedforms, but suggest that it is, on the basis of the similarity of the patterns observed in the 1986-1988 comparison.

The long wavelength bedforms identified in the field interact with the migrating chevrons in two ways. First, the stoss side of the long-wavelength bedforms provides a source for the minor component of lag granules that creates the dark chevrons seen in the Landsat images, and which are exposed on the surface in areas where the active sand sheet deposits are thin. Because the large-scale bedforms are cored by calcified pebble-gravel, these features most likely have not migrated during the time period studied; they may represent the planated core of what once were much greater amplitude giant ripples, like those that now occur east of the chevron area, and farther to the south (4). Second, the thickening of the planar stratified sand sheet deposits in the crest and lee of the large bedforms may be due to entrapment of individual layers of the sand sheet, formed as the light chevrons migrate downwind.

The rapid changes and lack of topography associated with the light chevrons suggest that their movement is restricted to a thin (0.5- to 2-cm) layer of the sand sheet. Despite such a thin layer, advance of 500 m per year of even a 1-cm thick individual light chevron equates to a bedform transport rate of 8.3 m^3 per year (12), or a net movement of $83,000 \text{ m}^3$ per year for a 10-km wide chevron. Continued monitoring of such features will allow more accurate estimates to be made of sand transport in large desert regions and will permit comparisons with mass movement derived from dunes and other smaller scale aeolian bedforms.

Fig. 6. Local topography and stratigraphy of large-scale bedforms in the sand sheet. (A) Short profile over 20-cm-high bedform showing thickening of active sand sheet in the crest and lee; (B) 2.7-km profile of chevron area: three long-wavelength (800 to 1200 m) bedforms have amplitudes of 15 to 30 cm, and are cored by calcified pebble-gravel (cpg). Total relief of this section is 60 cm, and only representative stratigraphy is shown based on 175 shallow pits. (C) Enlargement of large-scale bedform showing cpg core and thickening of active sand sheet deposits.



REFERENCES AND NOTES

1. R. A. Bagnold, *Geogr. J.* **82**, 103 (1933).
2. C. V. Haynes, Jr., and D. L. Johnson, *Geol. Soc. Am. Abstr. Prog.* **16**, 534 (1984); C. V. Haynes, Jr., *Science* **217**, 629 (1982) (north and south of Fig. 4B should be reversed); C. V. Haynes, Jr., *Quat. Res.*, in press.
3. C. V. Haynes, Jr., *Natl. Geogr. Soc. Res. Rep.* **16**, 269 (1984).
4. C. S. Breed, J. F. McCauley, P. A. Davis, *Geol. Soc. London Spec. Publ.* **35**, 337 (1987). Giant ripples occur with a regular spacing throughout much of the sand sheet, whereas the chevrons appear to be limited to localities downwind from scarps or major dune fields.
5. Routine destripping was done before geometric corrections on both 1972 (12 November 1972; identification number (ID) 1112-08083) and 1986 (4 January 1986; ID 5067407593) images, but was not necessary for the 1988 scene (16 October 1988;

ID 4228408025). Bilinear interpolation was used in resampling, and geometric correction resulted in 58-m rms error for the 1972 scene, 114-m rms error for the 1986 scene, and 41-m rms error for the 1988 scene. Overlay of the images in areas of bedrock ridges indicates that the registration is accurate to 1 to 2 pixels, although even in these areas, sand accumulations in the lee of bedrock ridges could make the coregistration appear worse than it actually is.

6. We converted the image data to spectral radiance following procedures outlined in B. L. Markham and J. L. Barker, [*Landsat Technical Notes 1* (Earth Observation Satellite Company, Lanham, MD, 1986)], in which

$$L_{\lambda} = LMIN_{\lambda} + \frac{LMAX_{\lambda} - LMIN_{\lambda}}{QCALMAX} QCAL$$

where L_{λ} is spectral radiance of band λ (in milliwatts per square centimeter per steradian per micrometer), $LMIN$ and $LMAX$ are calibrated spectral radiances used in ground processing, $QCALMAX$ is the range of radiance values, and $QCAL$ is the quantized scaled radiance value (dn) of the Landsat data. Exoatmospheric reflectance, ρ_p , was calculated by

$$\rho_p = \frac{\pi L_{\lambda} d^2}{ESUN_{\lambda} \cos \theta_s}$$

where d is the Earth-sun distances (in astronomical units), $ESUN$ is mean solar exoatmospheric reflectance (milliwatts per square centimeter per microm-

eter), and θ_s is solar zenith angle. Markham and Barker suggested that uncertainties in exoatmospheric reflectance resulting from sensor changes with time are less than 2% for the MSS instruments.

7. The brightness values thus calculated are essentially exoatmospheric reflectances, and although variation in reflectance between the scene dates can be caused by variations in aerosol composition, we assume that this composition was constant. Air temperature averaged 15° to 20°C at 0930 an (nominal Landsat pass time), and relative humidity was 20 to 30%. Sandstorms, which would completely obscure the surface from satellite observations, rarely occur from November to February.
8. A negative transparency from June 1985 was overlain on 1:1,000,000 prints from October 1984 and January 1986, and in each case, matching the chevron patterns produced offsets in the dune field to the west, and in bedrock exposures north of the sand sheet. We found this method of matching the chevron patterns and looking for changes in stable features more accurate than the reverse because there are only a few stable landforms in the region. When doing this, we noted no changes in the patterns of the chevrons, suggesting short-term (yearly) movement of the features as discrete bedforms.
9. The fine- to coarse-sand particles are dominantly iron oxide-coated quartz grains derived from the Nubian sandstone prevalent throughout the Western Desert of Egypt.
10. R. L. Folk, in *Proc. Intl. Geol. Cong. 23rd Session* (Academia, Prague, 1968), pp. 9-32; T. A. Max-

well, in *Desert Landforms of Southwest Egypt: A Basis for Comparison with Mars*, F. El-Baz and T. A. Maxwell, Eds. (Contractors Rep. 3611, National Aeronautics and Space Administration, Washington, DC, 1982), pp. 157-173.

11. R. Greeley and J. D. Iverson, *Wind as a Geological Process* (Cambridge Univ. Press, Cambridge, 1985), pp. 149-155; I. G. Wilson, *Sedimentology* 19, 173 (1972).
12. Bedform migration rate as defined by D. M. Rubin and R. E. Hunter [*Sedimentology* 29, 121 (1982)] is:

$$i = V H k$$

in which i is transport rate (volume per unit time per unit width), V is the rate of bedform migration, H is the bedform height, and k is cross-sectional area divided by wavelength divided by height.

13. We thank K. Katzer, B. Gillespie, and E.-S. Zaghlool for their assistance in surveying, and the General Petroleum Company, Egypt for logistical assistance during early phases of this study. This study was supported by National Science Foundation grants EAR-8312651 and EAR-8607479, National Geographic Society grant 2790-84, and Smithsonian Foreign Currency grant FC10215300 to C. V. H. and by the National Air and Space Museum, Smithsonian Institution to T. A. M. We thank P. A. Jacobberger, S. Soter, C. S. Breed, and two anonymous reviewers for their reviews of this manuscript.

31 August 1988; 22 December 1988